Nontrigonal Ge dangling bond interface defect in condensation-grown (100)$Si_{1-x}Ge_x/SiO_2$

A. Stesmans, P. Somers, and V. V. Afanas'ev
Department of Physics and Astronomy and INPAC, University of Leuven, 3001 Leuven, Belgium
(Received 12 February 2009; published 1 May 2009)

Multifrequency electron-spin-resonance (ESR) study has revealed a nontrigonal Ge dangling bond (DB)-type interface defect in $SiO_2/(100)Ge_xSi_{1-x}/SiO_2/Si$ heterostructures grown by the condensation method. The center, exhibiting monoclinic-I (C_{2v}) symmetry, with principal g values $g_1=2.0338\pm0.0003$, $g_2=2.038\,6\pm0.000\,6$, and $g_3=2.005\,4$ and lowest g value (DB) direction $24\pm2°$ off a $\langle111\rangle$ direction toward the [100] interface normal, is observed in maximum densities for $x\sim0.7$, the signal disappearing for $x\lesssim0.45$ and $x\gtrsim0.93$. Neither Si P_b type nor trigonal Ge dangling bond defects is observed, enabling unobscured spectral analysis. Based on its ESR parameters, including g matrix and symmetry, it is suggested to concern a Ge P_{b1}-type center, that is, not a trigonal basic Ge $P_{b(0)}$-type center ($Ge_3\equiv Ge^\bullet$), thus exposing a unique interface mismatch healing as function of substrate Ge fraction. Its properties are discussed within the context of the thus far elusive role of interfacial Ge DB defects in Ge insulator structures, encompassing theoretical inferences.

DOI: 10.1103/PhysRevB.79.195301 PACS number(s): 76.30.Mi, 73.20.Hb, 73.40.Qv

I. INTRODUCTION

The progress in deposited insulators of high dielectric constant κ required[1] in replacement of the conventional SiO_2 gate insulator in metal-oxide-semiconductor (MOS) electronics has risen the potential to surmount a key problem with a semiconductor such as Ge, i.e., in contrast with Si, the lack of a high-quality native insulator. This has led to a resurgence of interest in application of Ge where the better bulk electron (3900 vs 1400 cm^2/Vs) and hole (1900 vs 500 cm^2/Vs) mobilities over Si promise higher channel mobility, while the narrower band gap (0.67 eV at 300 K) enables reduced voltage operation, and hence, less power consumption.[2,3] A vital factor in successful MOS application is the ultimate quality of the semiconductor/insulator interface, where detrimental interface traps should be reduced to the (sub) 10^{10} cm^{-2} level, still a key issue[4] for Ge metal-oxide-semiconductor field-effect transistors (MOSFETs). In the case of thermal Si/SiO_2, a dominant role is played by the interfacial Si dangling bond (DB) defects, the archetypal P_b-type centers[5,6] as identified by electron-spin resonance (ESR), which fortunately can be efficiently passivated[7,8] by H [industrial anneal in forming gas ($\sim$10% H_2 in N_2)]. Yet, for Ge, achieving low interface trap density appears not straightforward.[4] Intense research has exposed basic differences[3,4,9,10] between the seemingly isomorphic interfaces Si and Ge would form with oxides. For one, ESR has so far failed to resolve interfacial Ge DB-type defects,[9] which leaves their occurrence and fate indistinct, implicit potential electrical activity—only paramagnetic defects residing in (near) interfacial dielectric layers have been detected; a dominant contribution to the interface trap spectrum comes from slow acceptor states resistant to thermal passivation by H. There appears the lack of fundamental insight.

Since there have been several suggestions for the failing ESR. On pure experimental side, it might just plainly concern insufficient ESR sensitivity, e.g., compared to Si, because of the excessive strain-induced g spread line broadening, resulting from the drastically enhanced ($\sim$6.6 times) spin-orbit (SO) coupling, so that defects at the sub-10^{12} cm^{-2} level could have remained undetected.[9] More fundamentally,[10] albeit contested in later work,[11] it has been concluded from first-principles density-functional theory on an isolated $^\bullet Ge\equiv Ge_3$ DB in c-Ge this defect to give rise to electronic levels below the valence-band (VB) maximum, resulting in exclusively negatively charged diamagnetic defects. Another view[12] may start from the origin of intrinsic P_b-type defects in Si/SiO_2 admittedly seen as inherent strain-induced defects to account for the interface mismatch[13] related to the $\sim$2.25 expansion in molar volume upon SiO_2 growth from Si. Here, compared to SiO_2, one may point to the higher "viscosity" of Ge oxide, which aided by the generally mixed phase (GeO; GeO_2) growth of thermal Ge oxide,[4,14–16] would render substantially more flexibility to the thermal Ge oxide in adopting to the c-Ge surface, thus drastically reducing the need for incorporation of as much mismatch adapting defects (to the sub-ESR-detection limit). Therefore, in an attempt to reveal Ge DBs, one might consider studying interfaces between Ge and a more robust oxide, e.g., SiO_2.

Notably though, there have been previous reports on the observation of a Ge DB defect by ESR, merely in less conventional semiconductor(/insulator) entities. As to pure c-Ge, early on, an X-band ESR signal at zero crossing g value $g_c=2.023$ of peak-to-peak derivative width $\Delta B_{pp}\sim50$ G was reported[17] as originating from the Ge DB at the c-Ge surfaces in powder of crushed c-Ge. Later, in a verifying K-band ESR experiment, such signal at $g_c=2.021$ with $\Delta B_{pp}\sim70$ G was detected[18] in powdered c-Ge. Recently, in an endeavor related to the current work, the present authors have observed a *structured* powder pattern in c-Ge implanted with Ge^+ (120 keV; dose $\sim1\times10^{15}$ cm^{-2}), which could be convincingly fitted by a powder pattern shape with $g_\parallel=1.999\,8$ and $g_\perp=2.026\,5$ using a Gaussian broadening function of $\Delta B_{pp}=45$ G. Early on, an X-band signal of $\Delta B_{pp}\sim39$ G at $g_c=2.021$ was observed[19] in rf sputtered a-Ge. Since, an impressive amount of ESR work[20] has been carried out on a-$Si_{1-x}Ge_x$:H alloys, reporting an isotropic

 ©2009 The American Physical Society

X-band signal at $g_c = 2.0175 - 2.022$ depending on manufacturing, of $\Delta B_{pp} \sim 47$ G in natural a-Ge and a-Ge:H prepared by electron-beam evaporation.

Two more works addressed X-band ESR on c-SiGe alloys. A basic one[21] reported on a first *anisotropic center* termed SG1, in annealed O-implanted(170–190 keV; dose $0.5-1.8 \times 10^{18}$ cm^{-2}) c-$Si_{0.9}Ge_{0.1}$ and c-$Si_{0.6}Ge_{0.4}$ alloys, showing $\langle 111 \rangle$ trigonal (C_{3v}) symmetry with $g_{\parallel} = 1.9998$, $g_{\perp} = 2.0260$, and $\Delta B_{pp\parallel} \sim 13$ G and $g_{\parallel} = 1.9985$, $g_{\perp} = 2.031$, $\Delta B_{pp\parallel} \sim 22$ G, respectively. It was ascribed to a threefold-coordinated central Ge atom backbonded to only Si or a combination of Si and Ge atoms situated at the interfaces of SiO_2 precipitates in the SiGe matrix. A second work[22] reported the observation of a Ge DB center termed Ge P_b, in weakly oxidized epitaxial porous $Si_{0.8}Ge_{0.2}$ layers of trigonal (C_{3v}) point symmetry, with $g_{\parallel} \sim 2.005$, $g_{\perp} = 2.021$ ($\Delta B_{pp\parallel} \sim 17$ G, $\Delta B_{pp\perp} \sim 28$ G), somewhat different from the previous work.

Here, we report on the ESR observation of a different Ge P_b-type interface defect in $(100)Si_{1-x}Ge_x/SiO_2$ heterostructures, herewith paving the way to assess the role of interfacial Ge DBs in device performance and test predictions. The absence of other overlapping paramagnetic signals enables reliable spectral analysis, unveiling a Ge DB defect of (less common) C_{2v} (monoclinic-I) symmetry, distinct from the anticipated axial symmetry of the elemental $^{\bullet}Ge \equiv Ge_3$ P_b defect.[21,22] Its atomic nature is addressed within the context of theoretical insight in defect occurrence.

II. EXPERIMENTAL DETAILS

Samples studied were $SiO_2/(100)Ge_xSi_{1-x}/SiO_2/(100)Si$ entities with atomic Ge fraction x in the range $0.45 \leq x \leq 0.93$ obtained through the condensation technique.[23,24] Briefly, this essentially implies a three-step process. It starts with epitaxially growing a $Si_{0.73}Ge_{0.27}$ layer (104 nm thick) on a Si(22 nm)/SiO_2/(100)Si silicon-on-insulator (SOI) substrate wafer. This is followed by capping with an epi-Si (6 nm), which is applied to prevent any Ge oxidation at the early stage of the thermal condensation process. Subsequent subjection to multistep (two or three) dry oxidation/inert ambient annealing at different temperatures (1150 °C, 1000 °C, and 900 °C) results in the formation of high-quality $SiO_2/Ge_xSi_{1-x}/SiO_2$ top structures with Ge-enriched SiGe layers, as evidenced by the results of a combination of top sensitive morphological/compositional sensitive analyzing techniques.

Measurement of the Ge content in the remaining SiGe layer by Rutherford backscattering spectroscopy shows that while the Ge fraction x may be increased by up to a factor 3, with an attendant gradual decrease in SiGe film thickness toward 29 nm for $x = 0.93$, the Ge atoms are not oxidized but effectively trapped between the two Si oxide layers formed. This is affirmed by Raman spectroscopy data. Much relevantly, cross-sectional transmission electron microscope (TEM) analysis indicates that the initial good crystal quality is maintained in the left Ge_xSi_{1-x} layers, showing two abrupt identical oxide/Ge_xSi_{1-x} film interfaces; while the TEM x-ray analysis points out uniform distribution of Ge throughout these layers. In addition, monitoring of the in-plane lattice constant $a_{\parallel}$ by high-resolution x-ray diffraction measurements reveals that the SiGe film relaxes as the condensation proceeds—the data being supported by Raman observations—pointing to a remaining strain in the $-0.9\% - -1.2\%$ range. More details can be found elsewhere.[24,25] Importantly, the applied thermal budget (900–1150 °C range) will leave no GeO_2 present.[14,15] The SiO_2 layers are essentially bare of Ge oxide.[14]

Conventional first harmonic multifrequency (X, K, and Q bands) ESR observations were carried out at 4.2 K. From the main samples, ESR-sized slices were cut of 2×9 mm^2 main area with the 9 mm edge along a $[0\bar{1}1]$ direction. Field angular-dependent measurements were carried out for the applied magnetic field **B** rotating in the $(0\bar{1}1)$ plane. The amplitude of the additionally applied modulation (~100 kHz) of the magnetic field and incident microwave power P_{μ} were appropriately reduced to avoid signal distortion. A comounted Si:P marker sample [$g(4.2\text{ K}) = 1.99869$] was used for accurate g value and defect density determination purposes. The latter was carried out through orthodox double numerical integration of either the directly detected first derivative-absorption curves $dP_{\mu r}/dB$ or computer simulations of these, where $P_{\mu r}$ is the reflected microwave power (see more details elsewhere).[8,13]

III. EXPERIMENTAL RESULTS AND ANALYSIS

Figure 1(a) shows a set of K-band ESR spectra observed for the applied magnetic field $\mathbf{B} \parallel \mathbf{n}$ ([100] sample normal) on samples of different Ge fraction x. For the range $0.54 \leq x \leq 0.73$, a prominent single signal is observed at $g_c = 2.0140 \pm 0.0003$ of $\Delta B_{pp} \sim 23$ G in varying intensity, reaching a maximum of $\sim 6.8 \times 10^{12}$ cm^{-2} per Ge_xSi_{1-x}/SiO_2 interface for $x \sim 0.7$. Noteworthy, apart from a weak isotropic EX center signal at $g_c = 2.00246$ ($\Delta B_{pp} = 3$ G)—an SiO_2 associated defect[26]—no other (interfering) signals, such as Si P_b-type interface centers, are observed, enabling reliable spectral analysis (unbiased by disentanglement issues) unlike the previous work.[21,22]

Angular variation for **B** rotating in the $(0\bar{1}1)$ plane reveals an anisotropic signal splitting into three in a closely 1:2:1 (in sequence of g_c) intensity ratio [cf. Fig. 1(b)]. Angular mapping, combining the results for all three ESR frequencies, resulted in the consistent three-branch g map shown in Fig. 2. Based on the archival knowledge[27] of encountered point defect symmetries in diamond crystal structures (Si), computer-assisted simulation reliably revealed a defect, with C_{2v} (monoclinic-I) symmetry and principal g values $g_1 = 2.0338 \pm 0.0003$, $g_2 = 2.0386 \pm 0.0006$, and $g_3 = 2.0054 \pm 0.0001$, with the lowest value g_3 direction $24 \pm 2°$ off a $\langle 111 \rangle$ direction toward **n** in the $(0\bar{1}1)$ plane ($31 \pm 2°$ off [100]). The inferred tensor orientation is sketched in Fig. 3(a). Only three branches (solid curves in Fig. 2) out of the seven expected for all equivalent defect orientations in a bulk diamond-type crystal are observed, indicating the *interfacial nature* of the defect. Independent direct evidence for the latter was provided through selective

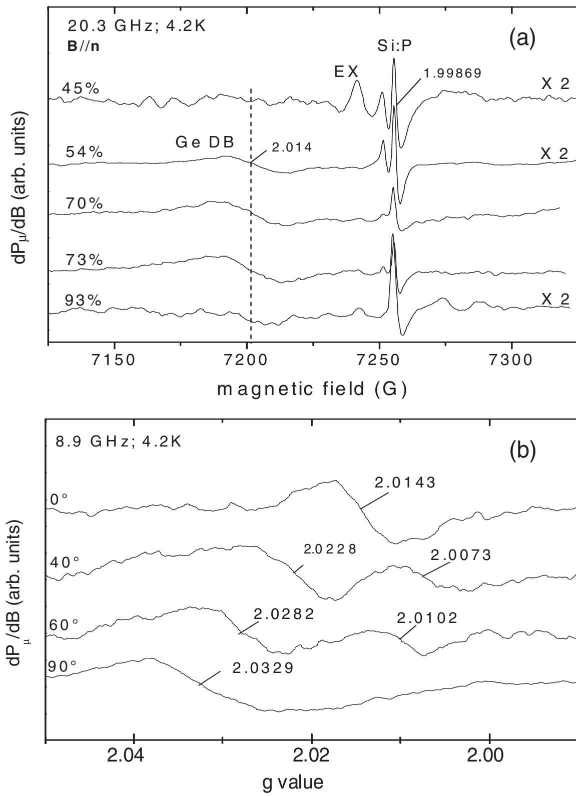

FIG. 1. First derivative-absorption *K*-band spectra of the Ge DB signal observed for $\mathbf{B}\|\mathbf{n}$ ([100] interface normal) on $(100)Si/SiO_2/Si_{1-x}Ge_x/SiO_2$ entities of different Ge fraction x (%). The signal at $g=1.998\,69$ stems from a comounted Si:*P* marker; (b) *X*-band ESR spectra measured ($x=0.7$ sample) for various angles of $\mathbf{B}$ with $\mathbf{n}$, showing the angular dependence.

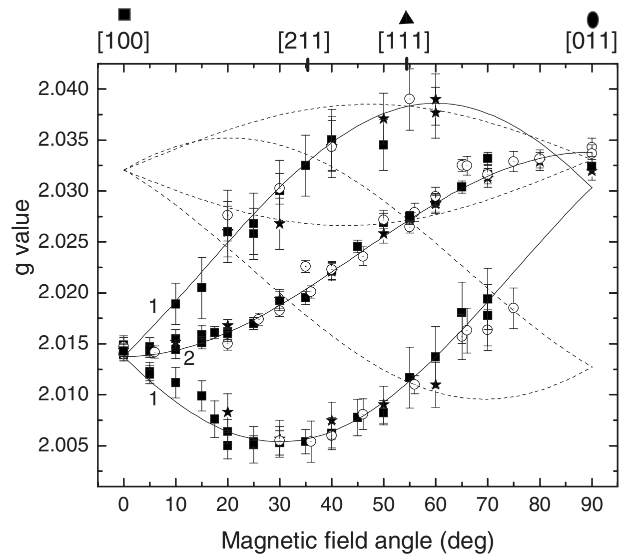

FIG. 2. Angular g map of G P_{b1} signals observed at three ESR frequencies [8.9 GHz (*), 20.3 GHz (■), 34 GHz (○)] on a $(100)Si/SiO_2/Si_{0.27}Ge_{0.73}/SiO_2$ entity for $\mathbf{B}$ rotating in the $(0\bar{1}1)$ plane. The solid curves represent the fitting result for monoclinic-I point symmetry of a defect in a Si (diamond) crystal, from where the principal g matrix values $g_1=2.033\,8\pm0.000\,3$, $g_2=2.038\,6\pm0.000\,6$, and $g_3=2.005\,4\pm0.000\,1$ are inferred. The dashed curve branches are not observed experimentally; only the four defect orientations equivalent through the $\bar{4}$-fold symmetry of the (100) face occur clearly exposing the interfacial nature of the originating defect. The added numbers to the branches indicate the relative intensities (area under absorption curves) of the corresponding ESR signals. The g_3 axis is at $31\pm2°$ off [100].

etching off the SiO_2 top layer in aqueous hydrofluoric acid of an $x=0.73$ sample, resulting in ~50% reduction in the ESR signal. The revealed defect symmetry is much reminiscent of that of the characteristic Si P_{b1} interface defect[28,29] in thermal $(100)Si/SiO_2$, from where it is provisionally labeled as G P_{b1}, since, as substantiated below, we are now dealing with an unpaired Ge bond signal.[30] In passing, we note that though the magnitudes of g values are comparable (as expected), the revealed C_{2v} symmetry and principle g axes orientations are well distinct from and exclude it to concern the trigonal (C_{3v}) defect previously observed in c-$Si_{1-x}Ge_x$ layers of low Ge fraction,[21,22] perhaps of the type $^{\bullet}Ge\equiv Si_3$.

Figure 4 shows the variation in the areal defect density per Ge_xSi_{1-x}/SiO_2 interface area as a function of ultimate Ge fraction x. The dotted curve suggests a Gaussian evolution.

Stepping from the consolidated knowledge for the P_b-type centers at the Si/SiO_2 interface,[5,7,8] additional insight as to the defect's nature may come from comparative study of the thermal defect-hydrogen interaction kinetics, i.e., passivation and depassivation, of much relevance in view of the potentially electrically detrimental character of the defect as well. Preliminary studies on an $x=0.73$ sample indicate that the G P_{b1} defects are successfully passivated in H_2 (1 atm, 500 °C, 1 h) by ~1 order of magnitude—yet not fully—to a residual density of $\sim4\times10^{11}$ cm^{-2}. For comparison, such thermal step would efficiently passivate Si P_b centers in ther-

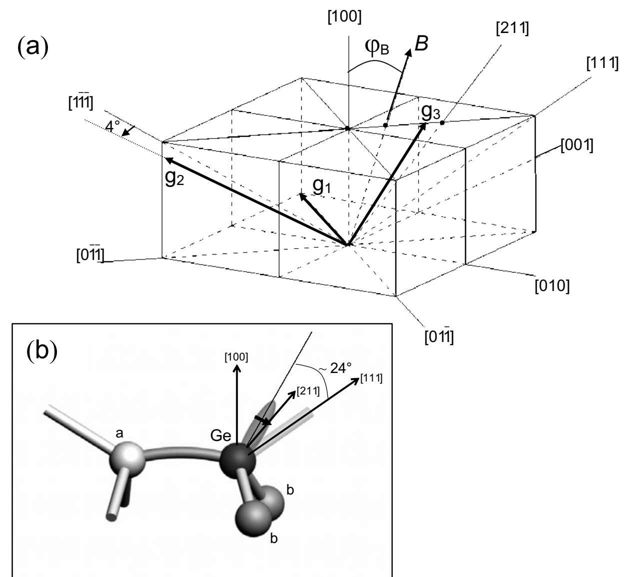

FIG. 3. (a). Schematic outline of the inferred g matrix orientation within the cubic Ge_xSi_{1-x} lattice for one of the possible four interface restricted equivalent defect orientations at the $(100)Ge_xSi_{1-x}/SiO_2$ interface; (b) proposed conceptual model for the observed interfacial G P_{b1} defect, where a and b may represent different (Ge and Si) atoms or all Ge atoms.

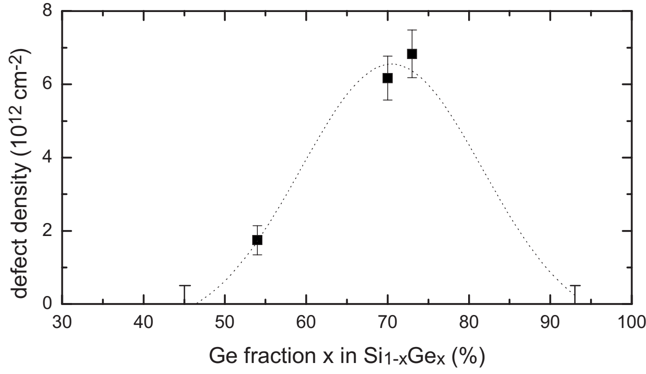

FIG. 4. Evolution of the GP_{b1} defect density per cm^2 of $Si_{1-x}Ge_x/SiO_2$ interface as a function of Ge fraction (x) of the central Ge_xSi_{1-x} layer inferred from ESR observations for **B**$\parallel$**n**. The detectivity limit is estimated at $\sim 1\times 10^{11}$ cm^{-2}. The fitted Gaussian curve guides the eye.

mal Si/SiO_2 to undetectable sub-10^{10} cm^{-2} levels.[7,8] The lower efficiency in the current $SiO_2/Ge_xSi_{1-x}/SiO_2/(100)$Si case may have resulted from the diffusion limitation on the needed lateral H_2 transport through SiO_2 over $\sim$1 mm in the studied 2-mm-wide slices.[31] Subsequent standard thermal depassivation treatment (vacuum, 605 °C, $\sim$40) fully restored the original GP_{b1} ESR signal, indicating reversal H passivation/depassivation kinetics as well known for Si P_b-type centers,[7,8] attesting to similar chemical reactions schemes. On the basis of the canonical insight on Si P_b centers[8] and previous Ge results,[32] the current highly successful passivation would counter the all-Ge symmetric $^{\bullet}Ge\equiv Ge_3$ entity as a possible model for the GP_{b1} center.

IV. DISCUSSION AND INTERPRETATION

A. Defect nature

The basic question arises as to the atomic nature of the defect revealed. Taking the view of an intrinsic interfacial DB defect, it could in principle concern an unpaired electron localized in a DB at a Si, Ge, or O atom, where the latter can be credibly excluded on grounds of previous ESR knowledge.[33] Stepping from the known g matrices of the $P_{b(0)}$ and P_{b1} interface Si DB defects,[6,28,29] closer g value consideration leaves little doubt GP_{b1} to concern a central Ge DB defect. Indeed, within a simple molecular-orbital consideration for Si or Ge of a DB defect with axial symmetry around the DB direction, simple SO theory alone predicts $g_{\parallel}=g_{fe}$ (=2.002 32, the free-electron g value), that is, no shift to first order, and $g_{\perp}$-$g_{fe}=\Delta g_{\perp}\propto\lambda$, the spin-orbit coupling constant. The g properties of GP_{b1} are well in line with the $\sim$6.6 times larger[34] λ of Ge than λ_{Si} (λ_{Ge}=940 cm^{-1}; λ_{Si}=142 cm^{-1}) [cf. $g_{\perp}$ (Si P_b) (Ref. 6) =2.008 8 vs $(g_1+g_2)/2\sim 2.036$ for GP_{b1}]. The Ge DB g values are affirmed by first-principles theory as well.[35]

This conclusion is firmly corroborated by the revealed dominant inhomogenous line broadening exhibiting a closely linear behavior, amounting to $\sim$1.13 G/GHz for **B**$\parallel$[100], resulting from a strain-induced spread σg in g—predominantly in $g_{\perp}$—as well known for the Si P_b-type defects at an interface or defects in amorphous (glass) environment. Values of σg (standard deviation) can be inferred to first order from fitting the width ΔB^G_{pp} of this Gaussian-type line broadening by the approximation[6]

$$\Delta B^G_{pp}(\theta)=\left(\frac{2hf}{g^3\beta}\right)(g_{\perp}\sigma g_{\perp}\cos^2\theta+g_{\perp}\sigma g_{\perp}\sin^2\theta), \quad (1)$$

where h is Planck's constant, β is the Bohr magneton, and θ is the angle of **B** with the corresponding sp^3-type DB direction (g_3), giving $\sigma g_{\perp}\sim 0.007$ 4, again $\sim\lambda_{Ge}/\lambda_{Si}$ times larger than $\sigma g_{\perp}$ ($\sim$0.000 85) of Si P_b in thermal[6] Si/SiO_2, as expected on grounds of λ.

A next step in defect identification entails the atomic backbond arrangement, chemically and physically, of the central defected Ge atom which—in principle based on material considerations—may involve Si, Ge, or O. As O diffuses from Ge at elevated temperatures[21] ($\geq$650 °C), Ge-O bonds are not expected to be part of the defect kernel. Next, the trigonal basic $^{\bullet}Ge\equiv Ge_3$ and $^{\bullet}Ge\equiv Si_3$ models simply appear excluded on grounds of revealed G P_{b1} symmetry, which, as to the former, is corroborated by the outlined results on passivation in H_2. Much informative here also is the observed defect density dependence on Ge fraction x (cf. Fig. 4). Noteworthy, what the data seem to indicate is that Ge P_b-type defect incorporation requires (as basic ingredient) the simultaneous presence of Ge, Si, and O atoms, as noted before.[21] Pertinently, no Ge DB signal is observed for $x\rightarrow 100\%$ ($\geq$93%), in compliance with previous ESR work on c-Ge/insulator structures.[9] The weakening defect density with decreasing x, to disappear below $x\sim 0.54$, i.e., with highest Si fraction, would once more disfavor the $^{\bullet}Ge\equiv Ge_3$ model. At intermediate Ge content, $0.54\leq x\leq 0.73$, the defect density increases along with the Ge content reaching a maximum at $x\sim 70\%$, i.e., where $\sim$3/4 of all alloys atoms are Ge atoms. Plain statistical considerations would then be in favor of the $^{\bullet}Ge\equiv Ge_2Si$ model and decline the other nonaxial possibility $^{\bullet}Ge\equiv GeSi_2$. In short, the assembled data so far, including explored thermal passivation behavior in H_2, would favor the $^{\bullet}Ge\equiv Ge_2Si$ model.

Yet, the above conclusion has been attained mainly on chemical (compositional) considerations. However, besides chemical dissimilarity among the backbonded atoms of a sp^3-type DB defect in a tetrahedral structure, lowering in g-matrix (defect) symmetry may also arise, as well known, structurally, i.e., atomic (bonding) arrangement. In fact, given the rather limited difference in bond length and strength between the Si-Ge and Ge-Ge bonds,[36] the former mechanism may not be at the origin. Staying within the semiconductor/insulator context, a prominent example of the latter case is the Si P_{b1} defect (of which, as remarked, the current GP_{b1} defect is much reminiscent), where within the currently adopted model of a defected interfacial Si-Si dimer, the monoclinic-I symmetry arises from variation in bond strength—and related—length among the three backbonded Si atoms, i.e., the $\equiv$Si–Si$^{\bullet}$=Si_2 model, where the long hyphen symbolizes a strained Si-Si (dimer) bond. So, objectively seen, a model with structurally induced asymmetry among the Ge backbonds may be feasible as well. However,

the observed disappearance of the GP_{b1} signal for $x \rightarrow 1$, may disfavor the latter. As synopsis, a conceptual defect model is suggested in Fig. 3(b).

Characteristically, the most powerful part of ESR spectroscopic information, almost exclusive in point defect identification[28,34] comes from resolved hyperfine (hf) structure arising from interaction of the unpaired electron with magnetic nuclei (isotopes) part of the immediate defect structure. But obviously, with no observation of resolved ^{73}Ge (I=9/2; 7.8% natural abundance; theoretical atomic hf interactions, obtained based on Hartree-Fock-Slater calculations with inclusion of a relativistic correction factor, at ^{73}Ge are about two times smaller than those at ^{29}Si, with $I=\frac{1}{2}$ and 4.67% abundance[34,37]) hf structure feasible by conventional ESR, final atomic assignment must await comparative first-principles theoretical analysis based on the provided g matrix values and symmetry, including the hinted DB direction (g_3). Fortunately, an accurate g matrix calculation has now become within reach.[35,38] In absence of such hf structure, no information on the sp^3-type orbital hybridization can be inferred either.

B. Defects absent

Another noteworthy observation of this work is the absence of Si P_b-type centers within experimental ESR sensitivity, including the sample with the highest Si fraction of ~55%. As already mentioned, it allows for unobscured reliable analysis of the presently revealed Ge-based defect. While perhaps coming with some surprise, we may note this finding not to be in conflict with previous work on O-implanted c-SiGe layers or epitaxial porous SiGe, where observed Ge P_b signals were found overwhelmed by intense Si P_b-type signals, as it is only reported for low x (≤ 0.2) values;[21,22] in the O-implantation work,[21] it has already been noticed that the Si P_b-type centers are virtually absent for higher x (=0.4). It refers to a common disappearance (below the ESR-detection limit) of Si $P_b s$ for x extending into the super 40% Ge fraction range. Here, one may suggest that in adapting the SiGe/SiO_2 interface mismatch, nature prefers to fix this exclusively, at least within ESR evidence, by formation of Ge DB-type centers, or—possibly—other ESR-invisible defects. One possible reason could be the ~21% larger bond strength of Si-O than Ge-O,[36] which would favor preferential breaking of the latter in a stressed environment.

As yet, no clear understanding of this effect has emerged. One may consider other possibilities. In a next view, one might hypothesize about the presence of a substantial second system of (near) interface defects, e.g., the revealed Ge P_{b1}-type centers, with relevant neutral ESR-active level energetically situated below that of Si P_b-type centers in the band gap. As the former system grows dominant with increasing x, the ESR-active Si P_b-type centers would gradually become ESR eluded as a result of charge exchange (depopulation). Clearly such interpretation will require the former system to outnumber the Si P_b system for $x \rightarrow 45\%$. But if we would consider the current Ge P_{b1}-type system as making up that former defect bath then if assuming a (minimum) density of P_{b0}, P_{b1} centers as found in[28] standard thermal Si/SiO_2, it means that for $x \rightarrow 70\%$, the density of G P_{b1} sites (including both ESR active and nonactive ones) would amount to $>1 \times 10^{14}$ cm^{-2}. As this may appear a quite unrealistic number, it would rather disfavor the current argument built on GP_{b1}-type centers. But of course, instead of the latter type of centers, the presumed second defect system may as well concern a different system of lower areal density that escapes ESR detection for inherent spectroscopic reasons (e.g., excessive line broadening). Such a system might occur here at the Ge_xSi_{1-x}/SiO_2 interface, while not at the different Si/SiO_2 interface.

We further notice that regardless of the Ge_xSi_{1-x}/SiO_2 interfaces, in particular there neither appears the stereotypic Si P_b-type signals from the buried oxide (BOX) SiO_2/Si substrate interface, generally expected for a "conventional" Si/SiO_2 interface, regardless of the layers on top. This is not ascribed to limited ESR sensitivity or unusual (different) choice of ESR spectroscopy parameters. Instead, it is seen as the natural result of the sample's thermal history including—among others—within the condensation procedure an annealing step at 1150 °C. As shown before for thermal (111)Si/SiO_2,[27] such step results in drastic reduction of Si P_b-type defects to sub-ESR detectivity levels, due to far-advanced relaxation ("viscous flow"), hence mismatch adaptation, of the (buried) SiO_2 layer in contact with the c-(100)Si substrate. The fact is a well-known aspect for state-of-the-art BOX structures, e.g., prepared by the separation by implantation of oxygen technique or bonded-and-etchback SOI method, implying extended annealing at temperatures in excess of 1100 °C.[39]

We also note that no "standard" trigonal Ge $P_{b(0)}$ signal $^{\bullet}$Ge≡Ge$_3$ is observed even for $x \rightarrow 100\%$, which leaves intact the theory adducing its basic ESR inactivity to it giving rise to electronic levels below the VB maximum. As it does not concern trigonal $^{\bullet}$Ge≡Ge$_3$, the observation of the GP_{b1} DB defect provides no (dis)proving power on this matter, including predicted highly inefficient passivation by hydrogen. Yet, it is quite feasible that the gradual disappearance of the revealed GP_{b1} defect *does touch* the very essence of the thus far elusive role of the interfacial Ge DB defects in the Ge/insulator edifice. Why, for $x \rightarrow 100\%$, no ESR-detectable interface defects are left at all? (For the $x \rightarrow 0\%$, Si P_b-type centers do appear). There may be various reasons. For one, starting from theory,[10] could it be that the theoretical inference advanced for the trigonal $^{\bullet}$Ge≡Ge$_3$ center apply (as well) for the current GP_{b1} defect, i.e., a matter of the defect's electronic levels descending into the VB in correlation with the band-gap narrowing with increasing x. Clearly then, the current data offer a test ground, where exact atomic defect identification will be prerequisite to enable theoretical assessment. As an interfacial Ge DB defect detected by ESR, it will potentially operate as a detrimental interface trap, with the degree of threat depending on the particular electron level(s) position in the band gap—insight which will require further combined studies of ESR and electrical analysis.

V. SUMMARY AND CONCLUSIONS

In summary, we have reported on the ESR observation of an unknown Ge P_{b1}-type defect in a semiconductor/insulator

structure, i.e., $(100)Si/SiO_2/Si_{1-x}Ge_x/SiO_2$. It is observed only in the range $0.54 \leq x \leq 0.73$, in varying intensities reaching a maximum for $x \sim 0.7$, to become undetectable for $x \leq 0.45$ and $x \geq 0.93$. With no other overlapping signals present, reliable g mapping together with g value considerations revealed an interfacial Ge DB defect of monoclinic-I (C_{2v})-type symmetry, with presumed DB orbital direction (g_3) $31 \pm 2°$ off [100] toward [111], atypical for the trigonal basic Ge P_b center ($^{\bullet}Ge \equiv Ge_3$) or $^{\bullet}Ge \equiv Si_3$. No Si P_b-type centers are observed.

The defect symmetry is much reminiscent of the Si P_{b1} center at the thermal $(100)Si/SiO_2$ interface. Based on the total of the experimental data, interfacial atomic structures $^{\bullet}Ge \equiv Ge_2Si$ or Ge-Ge$^{\bullet}$=Ge_2 with a strained Ge backbond are provisionally suggested models. In the absence of any resolved hf structure, necessary underpinning of the atomic assignment has to come from comparative evaluation from first-principles theoretical analysis mainly based on the provided g matrix values and symmetry,

No Ge P_b-type defect is observed for $x \to 100\%$, which complies with previous observations and theoretical inference. As noticed before regarding the observation of the trigonal Ge P_b center in crystalline environment, the observation of the current G P_{b1} defect requires the simultaneous presence of three ingredients at the interface, i.e., Ge, Si, and O, where one role of Si may be the realization of a Ge_xSi_{1-x}/SiO_2 interface with enhanced interfacial strain (mismatch) vis-à-vis that of Ge/GeO_x.

As the revealed Ge DB defect does not concern the trigonal Ge P_b ($^{\bullet}Ge \equiv Ge_3$) defect, its observation may elude direct relevance to current theory; yet the theory might be reiterated for the current G P_{b1} center to potentially account for its disappearance as ESR-active center for low Si fraction ($x \to 100\%$) with attendant band-gap narrowing.

ACKNOWLEDGMENTS

The authors are indebted to L. Souriau, R. Loo, and M. Meuris for providing samples as well as data on morphological analysis. They also acknowledge fruitful discussions with M. Houssa and G. Pourtois (IMEC). One of us (V.A.) was supported by the Fonds voor Wetenschappelijk Onderzoek (FWO)-Vlaanderen under Grant No. 1.5.057.07.

[1] See, e.g., G. D. Wilk, R. M. Wallace, and J. M. Anthony, J. Appl. Phys. **89**, 5243 (2001); J. Robertson, Eur. Phys. J. Appl. Phys. **28**, 265 (2004).

[2] C. O. Chui, S. Ramanathan, B. B. Triplett, P. McIntyre, and K. C. Saraswat, IEEE Electron Device Lett. **23**, 473 (2002).

[3] *Advanced Gate Stacks for High-Mobility Semiconductors*, edited by A. Dimoulas, E. Gusev, P. C. McIntyre, and M. Heyns (Springer, Berlin, 2007).

[4] D. Brunco *et al.*, J. Electrochem. Soc. **155**, H552 (2008).

[5] R. Helms and E. H. Poindexter, Rep. Prog. Phys. **57**, 791 (1994).

[6] A. Stesmans and V. V. Afanas'ev, J. Appl. Phys. **83**, 2449 (1998).

[7] K. Brower, Phys. Rev. B **38**, 9657 (1988).

[8] A. Stesmans, Appl. Phys. Lett. **68**, 2076 (1996); J. Appl. Phys. **88**, 489 (2000); J. Appl. Phys. **92**, 1317 (2002).

[9] V. V. Afanas'ev, Y. G. Fedorenko, and A. Stesmans, Appl. Phys. Lett. **87**, 032107 (2005).

[10] J. R. Weber, A. Janotti, P. Rinke, and C. G. Van de Walle, Appl. Phys. Lett. **91**, 142101 (2007).

[11] P. Broqvist, A. Alkauskas, and A. Pasquarello, Phys. Rev. B **78**, 075203 (2008).

[12] M. Houssa, G. Pourtois, M. Caymax, M. Meuris, M. M. Heyns, V. V. Afanas'ev, and A. Stesmans, Appl. Phys. Lett. **93**, 161909 (2008).

[13] A. Stesmans, Phys. Rev. B **48**, 2418 (1993).

[14] M.-A. Nicolet and W.-S. Liu, Microelectron. Eng. **28**, 185 (1995).

[15] K. Prabhakaran and T. Ogino, Surf. Sci. **325**, 263 (1995).

[16] S. R. Amy and Y. J. Chabal, in *Advanced Gate Stacks for High-Mobility Semiconductors*, edited by A. Dimoulas, E. Gusev, P. C. McIntyre, and M. Heyns (Springer, Berlin, 2007), p. 73.

[17] G. K. Walters and T. L. Estle, J. Appl. Phys. **32**, 1854 (1961).

[18] A. Stesmans and V. V. Afanas'ev, Microelectron. Eng. **80**, 22 (2005).

[19] M. H. Brodsky and R. S. Title, Phys. Rev. Lett. **23**, 581 (1969).

[20] See, e.g., M. Stutzmann, R. A. Street, C. C. Tsai, J. B. Boyce, and S. E. Ready, J. Appl. Phys. **66**, 569 (1989); T. Graf, T. Ishikawa, K. M. Itoh, E. E. Haller, M. Stutzmann, and M. S. Brandt, Phys. Rev. B **68**, 205208 (2003).

[21] M. E. Zvanut, W. B. Carlos, M. E. Twigg, R. E. Stahlbush, and D. J. Godbey, J. Vac. Sci. Technol. B **10**, 2026 (1992); Mater. Sci. Forum **83–87**, 1493 (1992).

[22] S. Lebib, M. Schoisswohl, J. L. Cantin, and H. J. von Bardeleben, Thin Solid Films **294**, 242 (1997).

[23] B. Vincent, J.-F. Damlencourt, P. Rivallin, E. Nolot, C. Licitra, Y. Morand, and L. Clavelier, Semicond. Sci. Technol. **22**, 237 (2007).

[24] V. Terzieva, L. Souriau, F. Clemente, A. Benedetti, M. Caymax, and M. Meuris, Mater. Sci. Semicond. Process. **9**, 449 (2006).

[25] L. Souriau, V. Terzieva, W. Vandervorst, F. Clemente, B. Brijs, A. Moussa, M. Meuris, R. Loo, and M. Caymax, Thin Solid Films **517**, 23 (2008).

[26] A. Stesmans, Phys. Rev. B **45**, 9501 (1992).

[27] C. A. J. Ammerlaan, in *Numerical Data and Functional Relationships in Science and Technology*, Landolt-Börnstein, edited by O. Madelung and M. Schultz (Springer, Berlin, 1987), Vol. 22, p. 365.

[28] A. Stesmans, B. Nouwen, and V. V. Afanas'ev, Phys. Rev. B **58**, 15801 (1998).

[29] A. Stirling, A. Pasquarello, J. C. Charlier, and R. Car, Phys. Rev. Lett. **85**, 2773 (2000).

[30] This label is consistent with a previous proposal made for a consistent scheme of labeling occurring ESR-revealed point defects at semiconductor/insulator interfaces, starting from historically first initiated labeling [A. Stesmans, Semicond. Sci. Tech-

nol. **4**, 1000 (1989) and Ref. 6], and in anticipation of potentially new emerging members as research advances. Depending on preference, one may prefer either the label GP_{b1} or GeP_{b1} for the current center.

[31] D. Griscom, J. Appl. Phys. **58**, 2524 (1985); B. J. Mrstik and P. J. McMarr, Phys. Rev. B **48**, 17972 (1993).

[32] S. M. Myers, H. J. Stein, and D. M. Follstaedt, Phys. Rev. B **51**, 9742 (1995).

[33] See, e.g., D. L. Griscom, in *Glass: Science and Technology*, edited by D. R. Uhlmann and N. J. Kreidl (Academic, New York, 1990), Vol. 4B, p. 151.

[34] W. Gordy, *Techniques of Chemistry XV* (Wiley, New York, 1980), p. 604.

[35] K. Sankaran, G. Pourtois, and M. Houssa, (unpublished).

[36] *CRC Handbook of Chemistry and Physics*, 83th ed. (CRC, Boca Raton, 2002), pp. 9–52.

[37] J. R. Morton and K. F. Preston, J. Magn. Reson. (1969-1992) **30**, 577 (1978); C. G. Van de Walle and P. E. Blöchl, Phys. Rev. B **47**, 4244 (1993).

[38] F. Neese, J. Chem. Phys. **122**, 034107 (2005); C. J. Pickard and F. Mauri, Phys. Rev. Lett. **88**, 086403 (2002).

[39] See, e.g., A. G. Revesz and H. L. Hughes, in *Physical and Technical Problems of SOI Structures and Devices*, edited by J. P. Colinge, V. S. Lysenko, and A. N. Nasarov (Kluwer, Dordrecht, 1995), p. 133.